

## Water Splitting Photovoltaic-Photoelectrochemical GaAs/InGaAsP - WO<sub>3</sub>/BiVO<sub>4</sub> Tandem Cell with Extremely Thin Absorber Photoanode Structure

S. Kosar<sup>1,\*</sup>, Y. Pihosh<sup>2</sup>, I. Turkevych<sup>3,4</sup>, K. Mawatari<sup>2</sup>, J. Uemura<sup>2</sup>, Y. Kazoe<sup>2</sup>, K. Makita<sup>3</sup>, T. Sugaya<sup>3</sup>,  
 T. Matsui<sup>3</sup>, D. Fujita<sup>4</sup>, M. Tosa<sup>4</sup>, Y. M. Struk<sup>1</sup>, M. Kondo<sup>3</sup>, T. Kitamori<sup>2</sup>

<sup>1</sup> Chernitsy National University, 101 Storozhynetska, 58000 Chernivtsy, Ukraine

<sup>2</sup> The University of Tokyo, 7-3-1 Hongo, Bunkyo, 113-8656 Tokyo, Japan

<sup>3</sup> National Institute of Advanced Industrial Science and Technology, 1-1-1 Umezono, 305-8568 Tsukuba, Japan

<sup>4</sup> National Institute for Materials Science, 1-2-1 Sengen, 305-0047 Tsukuba, Japan

(Received 30 May 2015; published online 22 August 2015)

We demonstrate highly efficient solar hydrogen generation via water splitting by photovoltaic-photoelectrochemical (PV-PEC) tandem device based on GaAs/InGaAsP (PV cell) and WO<sub>3</sub>/BiVO<sub>4</sub> core/shell nanorods (PEC cell). We utilized extremely thin absorber (ETA) concept to design the WO<sub>3</sub>/BiVO<sub>4</sub> core/shell heterojunction nanorods and obtained the highest efficiencies of photo-induced charge carriers generation, separation and transfer that are possible for the WO<sub>3</sub>/BiVO<sub>4</sub> material combination. The PV-PEC tandem shows stable water splitting photocurrent of 6.56 mA cm<sup>-2</sup> under standard AM1.5G solar light that corresponds to the record solar-to-hydrogen (STH) conversion efficiency of 8.1%.

**Keywords:** Photocatalysis, Photovoltaics, Renewable energy, Nanorods, WO<sub>3</sub>, BiVO<sub>4</sub>, Heterojunction.

PACS numbers: 84.60.Jt, 82.47.Jk, 88.40.jp,  
 88.40.jm, 82.45.Jn, 81.16.Hc, 81.07.-b

### 1. INTRODUCTION

Solar photovoltaics (PV) industry is growing rapidly and is going to achieve 235 gigawatts (GW) level of cumulative capacity installed worldwide by the end of 2015. This growth is stimulated by feed-in tariffs initiatives that were implemented by a number of governments in order to provide economic feasibility for investments into renewable energy. However, the distributed generation of electricity by residential PV

systems and commercial PV power plants is already causing instabilities of electric grid due to variability of the PV output. For that reason the storage of solar energy in a form of hydrogen that is generated via PV assisted photocatalytic water splitting is considered as a promising approach to compensate intermittency of the PV electricity supply with additional benefit of obtaining zero greenhouse gas emission fuel for transportation vehicles and aircrafts.

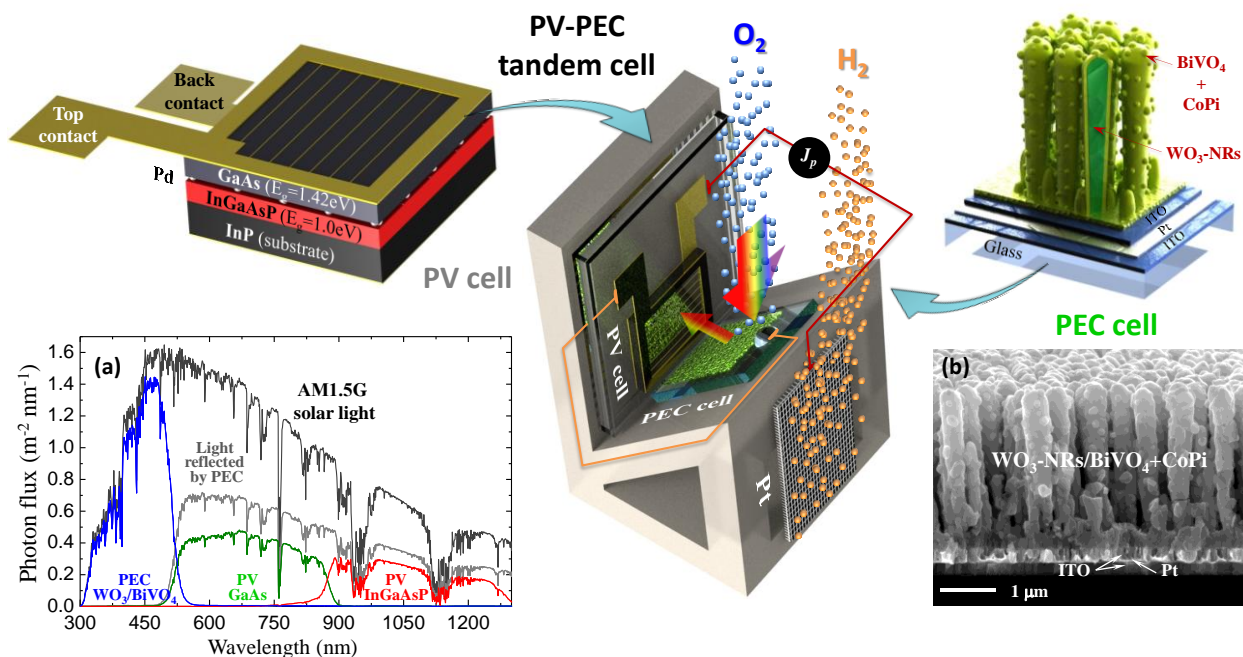


**Fig. 1** – Schematic illustration of the PV-PEC tandem device where the PV cell operates under reflected light from the PEC cell. (a) Utilization of the incident AM1.5G solar light by the tandem device that is calculated from external quantum efficiency (EQE) spectra of the PV-PEC tandem sub-cells. (b) Cross section SEM image of the PEC cell based on core/shell WO<sub>3</sub>/BiVO<sub>4</sub>+CoPi nanorods.

\* [sonya.kosar@gmail.com](mailto:sonya.kosar@gmail.com)

Since the discovery of photoelectrochemical water splitting on  $\text{TiO}_2$  by Fujishima and Honda [1], the photocatalytic decomposition of water by solar light has been considered as the most promising green technology for the generation of hydrogen. However, the solar-to-hydrogen conversion efficiency (STH) of  $\text{TiO}_2$  is fundamentally limited to 1.3% due to its wide band gap of 3.2 eV that allows utilization of the ultraviolet light only. Thus the development of photocatalytic materials with narrower bandgap that is sensitive to the visible part of the solar spectrum is highly desirable.

Bismuth vanadate ( $\text{BiVO}_4$ ) is one the most promising photocatalytic materials with direct bandgap of 2.4 eV and theoretical STH conversion efficiency of 9.2%. Unfortunately  $\text{BiVO}_4$  is characterized by a short carrier diffusion length ( $L_d$ ) of around 70 nm. As a result, the efficient generation of photocarriers is compensated by their fast recombination, which is the main reason for the unsatisfactory photocatalytic efficiency of  $\text{BiVO}_4$ . One possibility to compensate for the short  $L_d$  is to use an extremely thin absorber (ETA) heterojunction structure, where the  $\text{BiVO}_4$  absorber layer is thinner than the  $L_d$  while its optical thickness is reestablished by a structured configuration with a high aspect ratio (as illustrated in the Fig. 1).

In our previous work we have already demonstrated PEC cell with the ETA structure based on  $\text{WO}_3/\text{BiVO}_4$  core/shell nanorods with record water splitting efficiency approaching 8% in a self-biased water splitting PEC-PV tandem device [2]. In this work we report detailed characterization of the PV-PEC device and discuss mechanism of the water splitting process.

## 2. EXPERIMENTAL

We fabricated the PEC photoanode by a combination of glancing angle deposition (GLAD) of  $\text{WO}_3$ -NRs and electrochemical deposition (ED) of  $\text{BiVO}_4$  and cobalt phosphate co-catalyst. For the details about fabrication of  $\text{WO}_3$ -NRs by GLAD see our previous works [2, 3]. At first, we sputtered a three layer stack film of ITO (150 nm) / Pt (50 nm) / ITO (150 nm) on a fused silica substrate. The stack film had low sheet resistivity of  $4 \Omega/\square$  due to the encapsulated Pt layer. The Pt layer simultaneously functioned as a mirror reflector of the incident light. Then we changed the sample stage position to the GLAD regime with the deposition flux angle of  $85^\circ$  to the substrate normal and constant substrate rotation of 45 rpm. The  $\text{WO}_3$ -NRs with the length of 2.5  $\mu\text{m}$  were deposited by reactive sputtering at 0.3 Pa of  $\text{O}_2$  : Ar (9.6 : 11 sccm) working gas mixture and then crystallized by annealing in air at  $575^\circ\text{C}$  during 4.5 h. The  $\text{BiVO}_4$  layer with the thickness of 30 nm was electrodeposited over  $\text{WO}_3$ -NRs by the method of Seibold et al. [4] from 10 mM  $\text{Bi}(\text{NO}_3)_3$  in 35 mM  $\text{VOSO}_4$  electrolyte adjusted to pH = 4.7 at 0.21 V vs Pt counter electrode. Then the photoanodes were annealed in air at  $500^\circ\text{C}$  for 2 hours to obtain crystalline monoclinic  $\text{BiVO}_4$ . The cobalt phosphate (CoPi) co-catalyst was deposited on the  $\text{BiVO}_4$  surface by photo-assisted electrodeposition method according to the recipe of Li et al.[5].

The PV cell consisted of two mechanically stacked

GaAs ( $E_g = 1.42$  eV) and InGaAsP ( $E_g = 1.0$  eV) solar cells prepared by solid-state MBE followed by epitaxial lift-off (ELO) and then interconnected through aligned Pd nanoparticle arrays (Fig. 1) according to the previous works of Makita et al. [6, 7], Sugaya et al. [8, 9] and Mizuno et al. [10]. The PV cell was encapsulated by a glass cap and assembled on V-shape support with the PEC cell located at  $45^\circ$ . The performance of the PV-PEC tandem device was evaluated by following standard protocol for water splitting cells [11].

## 3. RESULTS AND DISCUSSION

Fig. 1 illustrates the concept of the PV-PEC tandem device and shows utilization of solar light calculated from external quantum efficiencies (EQE) of the PEC-PV tandem sub-cells. The cross-section and top-view SEM images in Fig. 1b and Fig. 2a,b reveal that GLAD formed well-separated  $\text{WO}_3$ -NRs with diameters of 150 ~ 200 nm. The subsequent ED of the  $\text{BiVO}_4$  layer proceeded in a "layer-plus-island" Stranski-Krastanov growth mode with formation of hemispherical clusters. The characteristic peaks in the XRD spectrum (Fig. 2c) confirm monoclinic phases of  $\text{WO}_3$  and  $\text{BiVO}_4$ .

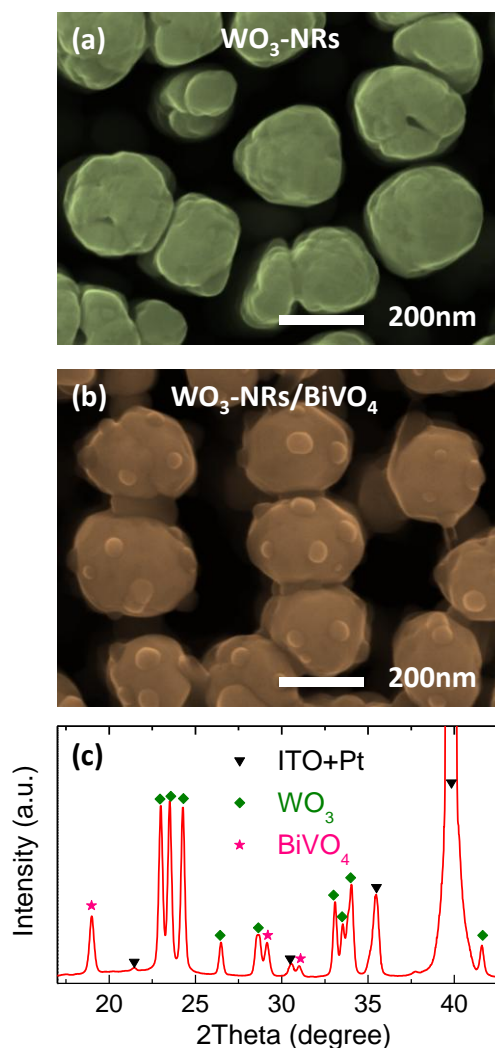
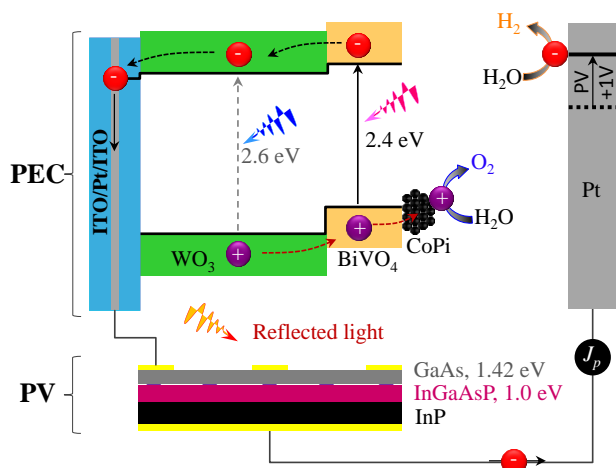


Fig. 2 – (a) and (b) show SEM images of  $\text{WO}_3$ -NRs and  $\text{WO}_3$ -NRs/ $\text{BiVO}_4$ , respectively, while (c) shows XRD spectrum of the ITO/Pt/ITO/ $\text{WO}_3$ -NRs/ $\text{BiVO}_4$  photoanode.

Fig. 3 shows schematic energy diagram of the  $\text{WO}_3\text{-NRs}/\text{BiVO}_4\text{+CoPi}$  photoanode and mechanism of the PV-assisted photocatalytic water splitting process. The solar light with the energy over 2.4 eV is mainly absorbed in the  $\text{BiVO}_4$  layer. Although  $\text{BiVO}_4$  layer is extremely thin, of around 30 nm, it is nevertheless very efficient absorber due to the direct bandgap of  $\text{BiVO}_4$  and enhanced light trapping in the high aspect ratio nanostructures. From a ray-optics perspective, the light trapping enhancement at rough interfaces is given by  $4n^2$ , where  $n$  is refractive index of the absorber layer [12]. Since the refractive index of  $\text{BiVO}_4$  is close to 2.5 [13] we can expect significant light trapping in the  $\text{BiVO}_4$  nanostructured layer. In contrast, the  $\text{WO}_3\text{-NRs}$  give small contribution to the overall light absorption due to indirect bandgap of  $\text{WO}_3$ . Thus the  $\text{WO}_3\text{-NRs}$  mainly function as highly conductive cores for the electron transport.



**Fig. 3** – Schematic energy diagram and mechanism of the PV-assisted photocatalytic water splitting by the  $\text{WO}_3\text{-NRs}/\text{BiVO}_4\text{+CoPi}$  photoanode.

The electron-hole pairs generated in the  $\text{BiVO}_4$  layer are separated at the  $\text{WO}_3/\text{BiVO}_4$  heterojunction interface that has type II band alignment. The electrons are effectively transferred to the ITO/Pt/ITO underlayer via highly conductive  $\text{WO}_3\text{-NRs}$  cores. The holes remained in the  $\text{BiVO}_4$  layer are transferred to co-catalyst CoPi clusters on the  $\text{BiVO}_4$  surface and participate in the oxygen evolution half-reaction (OER). The ETA structure of the core/shell  $\text{WO}_3\text{-NRs}/\text{BiVO}_4$  photoanode can be tuned to achieve near theoretical water splitting photocurrent by separate optimization of  $\text{WO}_3\text{-NRs}$  length and thickness of the  $\text{BiVO}_4$  absorber layer. In our case the optimized thickness of the  $\text{BiVO}_4$  layer was 30 nm that is more than two times thinner than the  $L_d$ . Simultaneously, the 2.5  $\mu\text{m}$  long core/shell  $\text{WO}_3/\text{BiVO}_4$  nanorods trap all the incoming light in the  $\text{BiVO}_4$  layer with the energy above its bandgap.

Spontaneous water splitting requires sufficient offsets of conduction and valence bands of the photocatalyst to provide suitable overpotentials for  $\text{H}_2$  and  $\text{O}_2$  evolution half-reactions. Unfortunately, the position of the  $\text{BiVO}_4$  conduction band does not fulfil that condition, and the photoanode needs an additional bias potential provided by a PV cell to drive the  $\text{H}_2$

evolution half-reaction. Previously, mechanically stacked tandems, based on a dye-sensitized solar cell (DSSC) with  $\text{Fe}_2\text{O}_3$  or  $\text{WO}_3$  photoanodes [14], and monolithic tandems, based on single- or double-junction a-Si solar cells with  $\text{BiVO}_4\text{:Mo+CoPi}$  photoanode layers [15], demonstrated self-biased photocurrents of 1.34, 2.23, 3.0 and 4.0  $\text{mA cm}^{-2}$ , respectively. In our case we used a double-junction GaAs/InGaAsP PV cell that operated under the light reflected from the photoanode. In this configuration, the portion of the solar light with the energy below 2.4 eV is transmitted to the Pt underlayer and then reflected toward the PV cell located at  $45^\circ$  with respect to the PEC photoanode.

The photoelectrochemical characterizations of the  $\text{WO}_3\text{-NRs}/\text{BiVO}_4\text{+CoPi}$  photoanode were conducted according to the standard characterization protocol for PEC cells [11] in potassium phosphate buffer solution (pH = 7) by a two electrode method with the bias applied vs Pt counter electrode. The simulated AM1.5G solar light was adjusted by using an NREL calibrated photodetector.

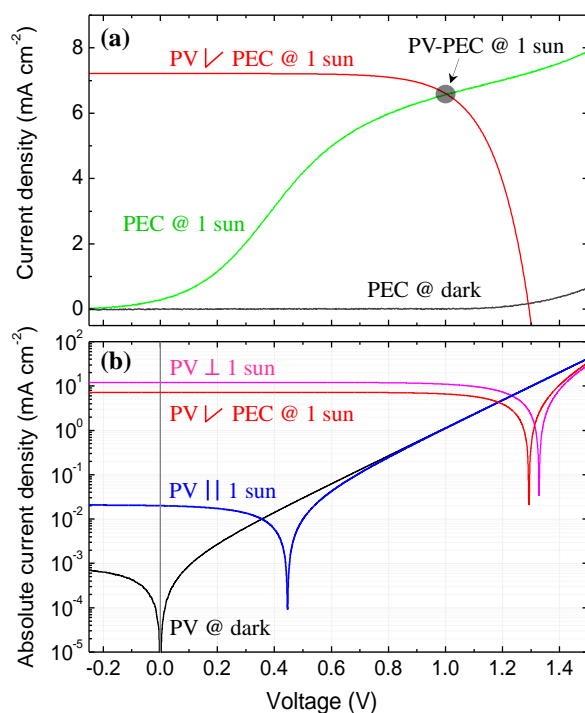


**Fig. 4** – (a) I-V characteristics of the PV cell (red) and the PEC cell (green) measured in the tandem configuration where the PV cell operated under the light reflected from the PEC cell. (b) I-V characteristics of the PV cell: (red) in the tandem configuration under the light reflected from the PEC cell, (blue) without the PEC cell in the tandem assembly, (black) at dark conditions and (pink) under normal incident light. The photocurrent is displayed in absolute values by using Log scale. All characterizations were performed by using standard AM1.5G light provided by a solar simulator with the light intensity calibrated to 1 sun.

The I-V characteristics of the PV and the PEC cells intersect around 1 V at 6.56 mA (Fig. 4a), which approaches 90% of the theoretically possible photocurrent value for  $\text{BiVO}_4$ . The STH efficiency of 8.1% is obtained by multiplying the photocurrent and the water splitting energy of 1.23 eV. To the best of our

knowledge, this is the highest up to date efficiency reported for water splitting PV-PEC tandems.

The PV and PEC cells with dimensions of 4 mm × 4 mm and 4 mm × 5.65 mm (i.e.  $\sqrt{2} \times 4$  mm), respectively, were assembled on a V-shape support in such a way that the PEC cell was located at 45° to the incident light while the PV cell was located parallel to the incident light. As a result the illuminated area of the tandem device was equal to 4 × 4 mm<sup>2</sup> and the PV cell operated only under the light reflected from the photoanode.

We also measured I-V characteristics of the PV cell without the PEC cell in the tandem assembly to confirm that the PV cell is oriented parallel to the incident light and does not receive additional light from parasitic reflections (Fig. 4b). Indeed, the I-V characteristics of the PV cell in the absence of the PEC cell in the tandem assembly were very close to the ones measured at dark conditions.

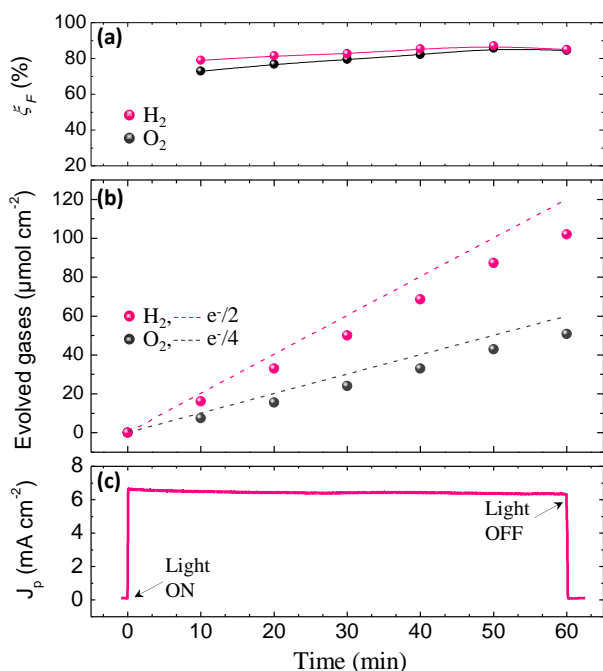


**Fig. 5** – (a) Faradaic efficiencies  $\xi_F$  and (b) specific quantities of evolved H<sub>2</sub> (red) and O<sub>2</sub> (black) gases per illuminated device area measured by gas chromatography with (c) simultaneously recorded photocurrent density  $J_p$ . The dashed lines correspond to the theoretical quantities of H<sub>2</sub> ( $e/2$ ) and O<sub>2</sub> ( $e/4$ ) gases that were calculated from the total charge by integrating the measured photocurrent  $J_p$ . The faradaic efficiencies  $\xi_F$  are calculated as ratios between the actually measured and the theoretically calculated quantities of the evolved gases.

In order to confirm that the measured photocurrent is utilized for the water splitting process, we directly measured the quantities of H<sub>2</sub> and O<sub>2</sub> evolved in an airtight reactor by gas chromatography. Fig. 5b shows specific quantities of evolved O<sub>2</sub> and H<sub>2</sub> gases while Fig. 5c shows simultaneously recorded photocurrent density. The H<sub>2</sub> and O<sub>2</sub> evolved at stoichiometric ratio with the H<sub>2</sub> generation rate approaching 102  $\mu\text{mol h}^{-1} \text{cm}^{-2}$ . The  $J_p$ -time profile was used to calculate the theoretical quantities of the evolved gases based on the total charge passed. Faradaic efficiencies ( $\xi_F$ ) were

calculated as ratios between the actually measured and the theoretically calculated quantities of the evolved gases. The faradaic efficiencies reach 80% within the first 15 minutes and later saturate at ~85%, which is a typical value for reactors with a single compartment, where the oxygen evolved from the photoanode can undergo a partial back reaction at the Pt counter electrode.

Fig. 1a reveals that the reflectance of the photoanode was only around 60% in the wavelength region >516 nm mainly due to the light scattering in the nanostructured photoanode. Nevertheless, the highly efficient GaAs/InGaAsP PV cell was able to generate the matching photocurrent even under the weak reflected light. Such high optical losses can be avoided in future by using a dichroic mirror that can split and guide dedicated portions of the solar spectrum separately to the PV cell and to the PEC cell.

The main advantage of the PV-PEC tandem configuration in comparison to the simple combination of PV cell and water electrolysis is the relaxed requirement for open-circuit potential of the PV cell. Direct electrolysis of water requires rather high overall potential of 1.6-2.0 V due to the high overpotential of oxygen evolution half-reaction that has to be compensated in addition the theoretical water splitting potential of 1.23 V. In contrast, our WO<sub>3</sub>-NRs/BiVO<sub>4</sub>+CoPi PEC cell requires a much lower bias of around 1 V that is in the range of recently developed inexpensive perovskite solar cells with open-circuit potential of 1.15 V [16]. The combination of a dichroic mirror and an inexpensive PV cell with ordinary performance characteristics can substitute expensive GaAs/GaAlAsP PV cell in the water splitting PV-PEC tandem device. Therefore, we believe that an economically viable PV-PEC tandem device based on a WO<sub>3</sub>-NRs/BiVO<sub>4</sub>+CoPi photoanode with STH of around 8% can be realized in the near future.

#### 4. CONCLUSIONS

In conclusion, we utilized an extremely thin absorber (ETA) concept to fabricate a highly efficient water splitting photoelectrochemical (PEC) cell based on core/shell WO<sub>3</sub>-NRs/BiVO<sub>4</sub>+CoPi and combined it in tandem device with double heterojunction GaAs/InGaAsP photovoltaic (PV) cell. The PV-PEC tandem device demonstrated ultimate water splitting photocurrent of 6.56 mA under simulated AM1.5G solar light that is close to 90% of the theoretically possible photocurrent for BiVO<sub>4</sub> and corresponds to the solar-to-hydrogen (STH) conversion efficiency of 8.1%. To the best of our knowledge, this is the highest water splitting efficiency reported up to the date among all PV-PEC tandem devices.

#### ACKNOWLEDGEMENTS

We acknowledge financial support from the Ivan Pulyui Scholarship Program of Ukraine, Core Research for Evolutional Science and Technology (CREST) program of the Science and Technology Agency (JST) of Japan and the New Energy Development Organization (NEDO) of Japan.

## REFERENCES

1. A. Fujishima, K. Honda, *Nature* **238**, 37 (1972).
2. Y. Pihosh, I. Turkevych, K. Mawatari, J. Uemura, Y. Kazoe, S. Kosar, K. Makita, T. Sugaya, T. Matsui, D. Fujita, M. Tosa, M. Kondo, T. Kitamori, *Nature Sci. Rep.* **5**, 11141 (2015).
3. Y. Pihosh, I. Turkevych, K. Mawatari, T. Asai, T. Hisatomi, J. Uemura, M. Tosa, K. Shimamura, J. Kubota, K. Domen, T. Kitamori, *Small* **10**, 3692 (2014).
4. J.A. Seabold, K.S. Choi, *J. Am. Chem. Soc.* **134**, 2186, (2012).
5. Y. Li, L. Zhang, A. Torres-Pardo, J.M. Gonzalez-Calbet, Y. Ma, P. Oleynikov, O. Terasaki, S. Asahina, M. Shima, D. Cha, L. Zhao, K. Takanabe, J. Kubota, K. Domen, *Nat. Commun.* **4**, 2566 (2013).
6. K. Makita, H. Mizuno, H. Komaki, T. Sugaya, R. Oshima, H. Shibata, K. Matsubara, S. Niki, *MRS Proceedings*, **1538**, 167 (2013).
7. K. Makita, H. Mizuno, R. Oshima, T. Sugaya, H. Komaki, K. Matsubara, *Photovoltaic Specialist Conference (PVSC), 2014 IEEE 40th*, 0495 (2014).
8. T. Sugaya, K. Makita, H. Mizuno, A. Takeda, T. Mochizuki, R. Oshima, K. Matsubara, Y. Okano, S. Niki, *Photovoltaic Specialist Conference (PVSC), 2014 IEEE 40th*, 0542 (2014).
9. T. Sugaya, K. Makita, A. Takeda, R. Oshima, K. Matsubara, Y. Okano, S. Niki, *Jpn. J. Appl. Phys.* **53**, 05FV06 (2014).
10. H. Mizuno, K. Makita, K. Matsubara, *Appl. Phys. Lett.* **101**, 191111 (2012).
11. Z. Chen, T.F. Jaramillo, T.G. Deutsch, A. Kleiman-Shwarscstein, A.J. Forman, N. Gaillard, R. Garland, K. Takanabe, C. Heske, M. Sunkara, E.W. McFarland, K. Domen, E.L. Miller, J.A. Turner, H.N. Dinh, *J. Mater. Res.* **25**, 3 (2011).
12. E. Garnett, P. Yang, *Nano Lett.* **10**, 1082 (2010).
13. J. Li, A. Bhalla, L. Gross, *Opt. Commun.* **92**, 115 (1992).
14. J. Brillet, J.-H. Yum, M. Cornuz, T. Hisatomi, R. Solarska, J. Augustynski, M. Graetzel, K. Sivula, *Nature Photon.* **6**, 824 (2012).
15. F.F. Abdi, L. Han, A.H. Smets, M. Zeman, B. Dam, R. van de Krol, *Nat. Commun.* **4**, 2195 (2013).
16. M. Grätzel, *Nat. Mater.* **13**, 838 (2014).